SLAC-PUB-10581
July 2004

Polarized Positrons at a Future Linear Collider and the Final Focus Test Beam

Achim W. Weidemann
Department of Physics, University of South Carolina,
Columbia, SC 29208, USA

For the E-166 Collaboration *

Having both the positron and electron beams polarized in a future linear e^+e^-collider is a decisive improvement for many physics studies at such a machine. The motivation for polarized positrons, and a demonstration experiment for the undulator-based production of polarized positrons are reviewed. This experiment ('E-166') uses the 50 GeV Final Focus Test electron beam at SLAC with a 1 m-long helical undulator to make $\approx 10 MeV$ polarized photons. These photons are then converted in a thin ($\approx$ 0.5 radiation length) target into positrons (and electrons) with about 50% polarization.

Submitted to the 32^{nd} International Conference on High-Energy Physics, ICHEP 04
16 - 22 August, 2004, Beijing, China

Stanford Linear Accelerator Center, Stanford University, Stanford, CA 94309

Work supported in part by Department of Energy contract DE-AC03-76SF00515.

POLARIZED POSITRONS AT A FUTURE LINEAR COLLIDER AND THE FINAL FOCUS TEST BEAM

ACHIM W. WEIDEMANN
Department of Physics, University of South Carolina,
Columbia, SC 29208
E-Mail: achim@SLAC.Stanford.EDU

FOR THE E-166 COLLABORATION*

Having both the positron and electron beams polarized in a future linear e^+e^-collider is a decisive improvement for many physics studies at such a machine. The motivation for polarized positrons, and a demonstration experiment for the undulator-based production of polarized positrons are reviewed. This experiment ('E-166') uses the 50 GeV Final Focus Test electron beam at SLAC with a 1 m-long helical undulator to make $\approx 10 MeV$ polarized photons. These photons are then converted in a thin (≈ 0.5 radiation length) target into positrons (and electrons) with about 50% polarization.

1 Introduction

Polarized positrons in e^+e^-collisions in addition to polarized electrons are a powerful tools for many physics studies, providing, e.g., increased effective polarization, signal enhancement and background suppression in a variety of physics processes, including supersymmetry and other new physics studies. Schemes to provide polarized positrons have been proposed a long time ago[1]. However it was often thought that production of polarized positrons was technically difficult, and initial proposals for future linear colliders assumed a conventional (or undulator-based) unpolarized positron source. In the last few years though, more attention was given to the physics case[2] for and technical feasibility of polarized positrons for e^+e^-colliders.

Polarized positrons can be produced by pair-production from circularly-polarized high-energy photons impinging on a target. In a case studied by a group in Japan, the circularly-polarized photons are made by Compton backscattering of a laser beam off a high-energy electron beam;[3] for future linear accelerator applications, though, the technical requirements on the pulsed laser system are extremely demanding. Another possibility is to use a helical undulator to make circularly-polarized high-energy photons. The latter method is particularly attractive for the proposed TESLA collider, which already uses a positron source based on pair-production from a (planar) undulator in its design.[4] Below I review the physics motivation for polarized positrons in high-energy e^+e^-collisions and then present a demonstration of undulator-based production of polarized positrons for future linear colliders in an experiment, E-166, which is now under way at the Stanford Linear Accelerator Center's Final Focus Test Beam (FFTB).

2 Physics Motivation

Having both beams polarized in a high-energy e^+e^-collider offers a number of advantages over the case of unpolarized positrons, among them a higher effective polarization, an increased signal to background ratio in studies of Standard Model processes or an enhancement of the effective luminosity; a more precise analysis of many kinds of non-standard couplings; improved accuracy of the polarization measurement, and the option to use transversely polarized beams, which again allow and improve certain measurements.

Details and examples of these effects are summarized in [2] and only some key points are highlighted here

2.1 Effective Polarization

In the study of the left-right asymmetry of s-channel vector particle exchange the effective polarization is defined as

$$P_{\rm eff} = \frac{P_{e^-} - P_{e^+}}{1 - P_{e^-} P_{e^+}} \,. \qquad (1)$$

The error of the measurement of the left-right asymmetry scales roughly with $1 - P_{\rm eff}$, favoring a high effective polarization. The final error on the asymmetries measured will in many cases be limited by the error on the polarization. Having both beams polarized significantly decreases the error on the effective polarization, as shown in Fig. 1.

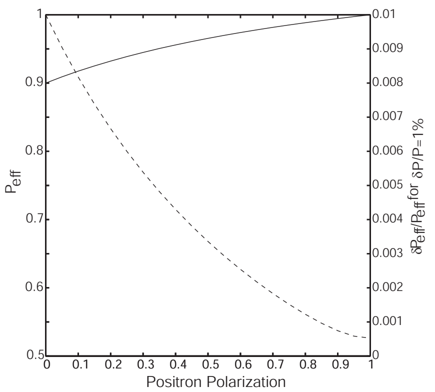

Figure 1. Solid curve/left scale (range: 0.5-1.0): the effective polarization (1) at a linear collider as a function of positron polarization (horizontal axis), assuming an electron polarization of 90%. Dashed curve/right scale (0.00-0.01): the relative error in the effective polarization $\delta P_{eff}/P_{eff}$, assuming $\delta P_{e-}/P_{e-} = 1\%$.[11]

2.2 Standard Model Physics

Standard Model physics based on WW or ZZ production depends on the effective polarization of the two lepton beams. This can be used to either enhance or suppress the standard model processes. As the dominant background processes for many new physics searches are WW and ZZ production, suppressing their contributions can enhance the search potential for new physics. For example, a positron polarization of about $P_{e^+} = -60\%$ would double the suppression of the WW background compared to $P_{e^+} = 0\%$ (assuming $P_{e^-} = 80\%$ in both cases).

2.3 Enhancement of Effective Luminosity

In Standard Model s-channel processes, due to its (V$-$A) couplings, only the (LR) and (RL) configurations of the initial $e^\pm$ contribute. The fraction of colliding particles is therefore

$$\frac{1}{2}(1 - P_{e^-} P_{e^+}) \equiv \frac{\mathcal{L}_{\rm eff}}{\mathcal{L}} \,, \qquad (2)$$

which defines an effective luminosity $\mathcal{L}_{\rm eff}$. If both beams are polarized,with *e.g.* $P_{e^+} = 60\%$, $P_{e^-} = -80\%$, this $\mathcal{L}_{\rm eff}$ is 0.74 compared to 0.5 for $P_{e^+} = 0\%$ and any P_{e^-}.[2]

2.4 Physics beyond the Standard Model

Supersymmetry (SUSY) is a leading candidate for new physics. However, even the simplest version, the Minimal Supersymmetric Standard Model (MSSM), leads to 105 new free parameters. If SUSY exists, one of the most important studies to be performed will be the determination of the SUSY parameters in an as model-independent way as possible and to prove the underlying SUSY assumptions, e.g., that the SUSY particles carry the same quantum numbers (with the exception of spin) as their Standard Model counterparts.

For example, SUSY transformations associate chiral (anti)fermions to scalars $e^-_{L,R} \leftrightarrow \tilde{e}^-_{L,R}$ but $e^+_{L,R} \leftrightarrow \tilde{e}^+_{R,L}$. Both beams have to be polarized in order to prove these associations. [5] The process $e^+e^- \to \tilde{e}^+\tilde{e}^-$ occurs via γ and Z exchange in the s-channel and via neutralino $\tilde{\chi}^0_i$ exchange in the t-channel. The association can be directly tested only in the t-channel and the use of polarized beams serves to separate out this channel. Fig. 2 shows an example of this; here the selectron masses are assumed to be close together, $m_{\tilde{e}_L} = 200$ GeV, $m_{\tilde{e}_R} = 190$ GeV, so that $\tilde{e}_L$, $\tilde{e}_R$ decay via the same decay channels (other SUSY parameters are taken from the reference scenario SPS1a[6]). The $\tilde{e}_L^-\tilde{e}_R^+$ pair can be enhanced by the LL configuration of the initial beams. From Fig. 2, it is seen that just having the electron beam polarized will not help. With $P_{e^-} = -80\%$, $P_{e^+} = 0\%$ the cross section for the combinations $\sigma(\tilde{e}_L^-\tilde{e}_R^+) = 102$ fb and $\sigma(\tilde{e}_L^-\tilde{e}_L^+) = 108$ fb are close together. This will essentially not change even if $P_{e^-} = -100\%$ were available.

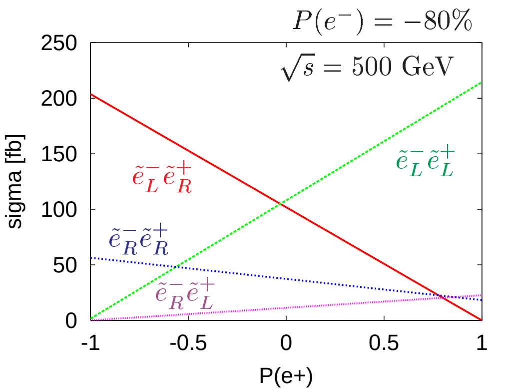

Figure 2. Separation of the selectron pair $\tilde{e}_L^-\tilde{e}_R^+$ in $e^+e^- \rightarrow \tilde{e}_{L,R}^-\tilde{e}_{L,R}^+$ with longitudinally polarized beams in order to test the association of chiral quantum numbers to scalar fermions in SUSY transformations.[2]

However, if polarized positrons are available, a separation of the different combinations might be possible.

For many SUSY analyses other SUSY processes are the most important background. Positron polarization can again be used to suppress the undesired process, as illustrated for selectron production in [7].

2.5 *Transversely Polarized Beams*

Recently, theoretical interest has increased into the physics opportunities transversely polarized lepton beams offer. The cross section involving transversely polarized leptons is given by

$$\sigma = (1 - P_{e^+}P_{e^-})\sigma_{\text{unpol}} + (P_{e^-}^L - P_{e^+}^L)\sigma_{\text{pol}}^L + P_{e^-}^T P_{e^+}^T \sigma_{\text{pol}}^T. \quad (3)$$

Access to the physics of the transverse cross section σ_{pol}^T requires therefore that both beams be polarized.

It has been shown in [10] that transversely polarized beams project out $W_L^+W_L^-$ final states, which are particularly important for studying the origin of electroweak symmetry breaking. When studying the azimuthal asymmetry, which is very pronounced at high energies, reaching about 10% , and peaks at larger angles, one has direct access to the LL mode of WW production without complicated final-state analyses.

The azimuthal asymmetry is also a crucial observable when studying signals of extra dimensions in the process $e^+e^- \rightarrow f\bar{f}$.[9] With the use of transversely polarized beams it is possible to probe spin-2 graviton exchange to about twice the sensitivity of "conventional" methods for analyzing contact interactions. In Fig. 3, the differential azimuthal asymmetry distribution is shown; its asymmetric distribution is the signal for the graviton spin-2 exchange.

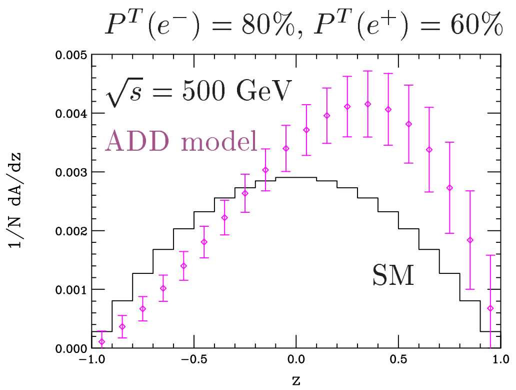

Figure 3. Search for large extra dimensions in the ADD model in $e^+e^- \rightarrow f\bar{f}$ with transversely polarized beams. Shown is the differential azimuthal asymmetry distribution whose asymmetric distribution is the signal for the graviton spin-2 exchange.[9]

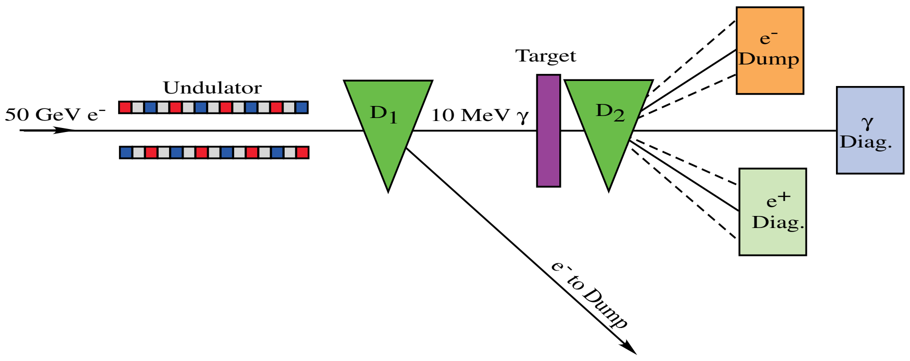

Figure 4. Conceptual layout (not to scale) of the experiment. 50-GeV electrons enter from the left and pass through an undulator to produce a beam of circularly polarized photons of MeV energy. The electrons are deflected away from the photons by the D_1 magnet. The photons are converted to electrons and positrons in a thin target. The polarizations of the positrons, and of the photons, are measured in polarimeters based on Compton scattering of photons in magnetized iron.

2.6 Precision Measurement of Beam Polarization

A Linear Collider operating at energies around the Z^0 pole is a very powerful instrument to probe the precision structure of the standard model. Beam polarization contributes greatly to the physics potential of this option. In order to exploit this physics potential, an extremely precise knowledge of the degree of polarization is needed. At the moment no method exists to directly measure the beam polarization to well below 0.1%.

However if both the electron and the positron beams are polarized, the degree of polarization can be measured from the events themselves. In this so-called extended Blondel scheme the left-right asymmetry is directly measurable from observing counting rates for all four possible combinations of polarizations, (+,+),(+,-),(-,+), and (-,-) for the two (e^+,e^-) beams. With this scheme an accuracy of the electroweak mixing angle of $\delta(\sin^2\theta_{\rm eff}) = 0.00001$ and $\delta(M_W) = 6$ MeV seems possible.[11]

3 E-166

The experiment E-166 at the SLAC Final Focus Test Beam (FFTB) is designed to test undulator-based production of polarized positrons for a future high-energy linear collider.[12] In this experiment, the low-emittance 50 GeV FFTB electron beam will pass through the bore of a one-meter-long helical undulator to generate circularly-polarized photons of a few MeV, which are then converted in a thin target to generate longitudinally-polarized positrons by pair-production. The positrons are then selected by a magnetic spectrometer, and their polarization measured, as described below.

Many parameters of this experiment are similar to those actually required at a future linear collider, except, of course, for total undulator length and electron beam energy E_e, and the number of positrons produced per pulse, as shown in Table 1.

3.1 Photon Production and Undulator Design

For the production of the polarized photons, the 50 GeV FFTB electron beam is passed through the center bore of a 1-m long helical undulator. This undulator consists of 0.6-mm diameter copper wire bifilar helix, wound on a stainless steel support tube with inner diameter 0.89 mm.

The photons generated in the undulator

Table 1 TESLA, NLC, E-166 Parameters

Parameter	TESLA	NLC	E-166
Beam Energy E_e[GeV]	150-250	150	50
N_e/bunch	3×10^{10}	8×10^9	1×10^{10}
N_{bunch}/pulse	2820	190	1
Pulses/s [Hz]	5	120	30
Undulator Type	planar	helical	helical
Undulator Parameter K	1	1	0.17
Undulator Period λ_u [cm]	1.4	1.0	0.24
Undulator Length L [m]	135	132	1
First Harmonic Cutoff, E_{c10} [MeV]	9-25	11	9.6
dN_γ/dL [γ/m/e^-]	1	2.6	0.37
Target Material	Ti-alloy	Ti-alloy	Ti-alloy,W
Target Thickness[Rad.Length]	0.4	0.5	0.5
Yield e^+/photon [%]	1-5	1.5	0.5
Positrons/bunch	3×10^{10}	8×10^9	2×10^7
Positron Polarization [%]	–	40-70	40-70

TESLA: unpolarized TESLA positron source,[4]; NLC: proposed polarized positron source

can be understood as the result of backscattering of the electron beam off the virtual photons of an undulator of period λ_U. Photons of a few MeV are needed to allow pair-production of positrons, requiring the highest available electron beam energy E_e, and the shortest undulator period λ_u

The flux of the generated photons is proportional to the density of the virtual undulator photons, or equivalently, to the square of the magnetic field, which is commonly measured by the dimensionless undulator parameter $K = 0.09 B_0[T]\lambda_U[mm]$. We choose $\lambda_U = 2.4mm$ and $K = 0.17$ for our undulator, which has an inner bore of $0.89mm$, (less than λ_U,) to obtain a sufficient field strength ($B = 7.6kG$ for a 2300 A current). Fortunately, the excellent FFTB beam has a low emittance ($\gamma\epsilon_x = \gamma\epsilon_y = 3 \times 10^{-5}m$-$rad$) and small rms beam size ($40\mu meter$) so that it will pass through the bore (11 times rms beam size) without scraping; but careful beam tuning will be required.

The expected intensity is then

$$\frac{dN_\gamma}{dL} = \frac{30.6}{\lambda_u[\mathrm{mm}]}\frac{K^2}{1+K^2}\ \mathrm{photons/m}/e^-$$
$$= 0.37 \mathrm{photons/m}/e^-. \quad (4)$$

The photon number spectrum is relatively flat up to the maximum energy of first harmonic radiation, E_{c10}:

$$E_{c10} \approx 24\ [\mathrm{MeV}]\frac{(E_e/50[\mathrm{GeV}])^2}{(\lambda_u[\mathrm{mm}](1+K^2))} = 9.6MeV. \quad (5)$$

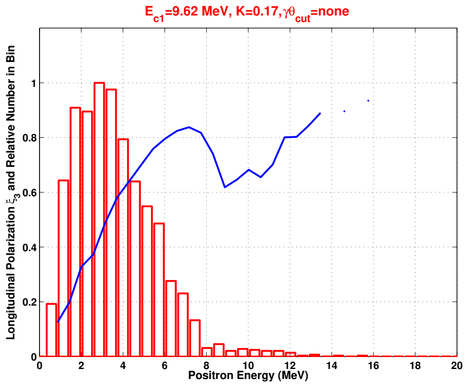

Figure 5. Longitudinal polarization (solid curve) and energy spectrum (histogram) of positrons emitted (Horizontal scale: positron energy, range: $0 - 20MeV$). The solid line is polarization averaged over a 0.5-MeV energy slice. The dip in the polarization at 9 MeV is due to the corresponding dip in photon polarization at about 10 MeV.

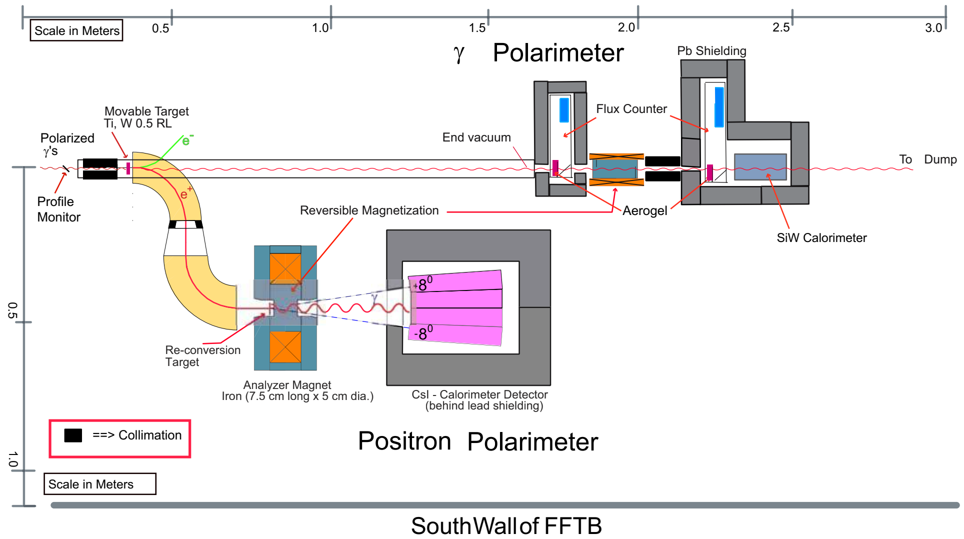

Figure 6. Conceptual layout of the E–166 positron generation and photon and positron diagnostic systems. Photon beam enters from top left, if no target is inserted, it continues to the photon polarimeter (in upper right of Figure); if the target is inserted, the produced positrons are transported (downward in Figure) to the positron polarimeter.

3.2 Positron Production

When a circularly polarized photon creates an electron-positron pair in a thin target, the polarization state of the photon is transferred to the outgoing leptons.[13] Positrons with an energy close to the energy of the incoming photons are 100% longitudinally polarized, while positrons with a lower energy have a lower longitudinal polarization.

Energy loss of positrons by bremsstrahlung in a target is accompanied by a slight loss in polarization, while low-energy positrons ($< 1MeV$) are stopped by ionization loss even in thin targets. These effects and simulation studies indicate that a target of about 0.5 radiation lenghts delivers positrons of the highest polarization for a given energy.

Figure 5 gives the longitudinal polarization (solid curve) and energy spectrum (histogram) of positrons emitted from a 0.5-radiation-length-thick Titanium target irradiated with photons of the energy and polarization spectra for the chosen undulator design. The polarization of the total sample is about 53%. The conversion efficiency from low-energy γ-rays to positrons in a thin target is about 0.5%.

3.3 Polarimetry

The measurement of the circular polarization of high-energy photons is based on the spin dependence of Compton scattering off atomic electrons. In this experiment, the transmission of unscattered photons through a thick magnetized iron cylinder is used.[14] (Scattering removes photons from the flux.) The spin-dependent part of the Compton cross section is $P_\gamma P_e \sigma_p$, where P_γ is the net photon polarization, P_e the net polarization of the atomic electrons ($\pm 7.92\%$ for saturated iron), and σ_p is the polarized part of the Compton scattering cross section. Then, the transmission probability has a polarization-dependent term, $T^{\pm}(L)$:

$$T^{\pm}(L) \approx exp[\pm nLP_\gamma P_e \sigma_p]. \qquad (6)$$

where n is the number density of atoms in iron, and L the length of the absorber. The $+$ or $-$ in $T^{\pm}(L)$ indicates if the electron spin in the iron is parallel or antiparallel to the direction of the incident photons. The asymmetry of the photon flux (1-6 %) for the two iron magnetization directions is then proportional to the photon polarization.

While an iron absorber of about 8 cm thickness is optimal for 7.5 MeV photons, a thickness of about 15 cm is best in the presence of backgrounds.

The photon polarimeter, shown in the upper part of Fig. 6, includes an aerogel Cerenkov detector before and after the magnetized iron absorber, and a total-absorption Silicon-Tungsten (SiW) sampling calorimeter. The areogel detectors are only sensitive to photons with an energy above $\approx 5MeV$; therefore, they give a photon number asymmetry independent of lower-energy photon backgrounds, while the SiW calorimeter records the energy-integrated photon spectrum and energy-weighted asymmetry.

When the positron production target is inserted into the undulator photon beam line, the produced positrons are collected and displaced from the photon beam by a positron transport line, with an efficiency of about 2%.

The polarization of these positrons is then measured by a two-step process; first, they are reconverted by a $0.175cm$-thick Tungsten target into polarized photons, and then the polarization of these photons is measured, again by transmission polarimetry through a magnetized iron cylinder, as discussed above. The emerging photons, with a typical energy of about 1 MeV, and about 1000 per pulse, are then measured in a CsI crystal calorimeter.

Geant simulations have shown that systematic errors in the polarization measurements are of the order of $\Delta P/P \approx 5\%$; they are dominated by the (limited) knowledge of the effective polarization of the atomic electrons in the iron. More details can be found in [12].

4 Summary and Outlook

Since its approval in June 2003, the E-166 Experiment has already undertaken background studies, and undulator fabrication is under way. At this time (August 2004) the installation of the components for E-166 and detector operation for background studies is under way; the experiment proper is scheduled to run in October 2004 and January 2005. Obtaining and measuring of positron polarization of better than 50 % will demonstrate the feasibility of undulator-based production of polarized positrons for a future linear collider, where ever it may be built and whatever choice of linear accelerator technology, warm or cold, is made.

Acknowledgements

I would like to thank all my colleagues on E-166 for an enjoyable and fruitful collaboration. This work was supported by the U.S. Department of Energy under Contracts DE–FG02–95ER40910 (SC) and DE-AC03-76SF00515 (SLAC).

References

1. V.E. Balakin and A.A. Mikhailichenko, Budker Institute of Nuclear Physics, *Preprint BINP 79-85* (1979).
2. G. Moortgat-Pick and H. Steiner, *EPJdirect* **C6**, 1 (2001), DESY-00-178.
3. T. Hirose, K. Dobashi, Y. Kurihara, T. Muto, T. Omori, T. Okugi, I. Sakai, J. Urakawa, M. Washio, *Nucl.Instr.Meth.* **A455**, 15 , 2000.
4. R. Brinkmann *et al.*, TESLA Technical Design Report, *Report DESY 2001-11*, March 2001.
5. C. Blochinger, H. Fraas, G. Moortgat-Pick and W. Porod, *Eur. Phys. J. C* **24**, 297 (2002), hep-ph/0201282.

6. B.C. Allanach *et al.*, *Proc. of the APS/DPF/DPB Summer Study on the Future of Particle Physics (Snowmass 2001)* , ed. by N. Graf, *Eur. Phys. J. C***25**, 113 (2002).
7. M. Dima *et al.*, *Phys. Rev. D* **65**, 071701 (2002).
8. See also the links on `http://www.ippp.dur.ac.uk/~gudrid/power/`.
9. T. G. Rizzo, *JHEP* **0302**, 008 (2003).
10. J. Fleischer, K. Kolodziej, F. Jegerlehner, *Phys. Rev. D***49**, 2174 (1994).
11. R. Hawkings and K. Mönig, EPJdirect C, Vol. 1, **C8**, 1 (1999); K. Mönig, LC–PHSM–2000–059; J. Erler, S. Heinemeyer, W. Hollik, G. Weiglein and P. M. Zerwas, *Phys. Lett. B***486**, 125 (2000).
12. G. Alexander *et al.*, Undulator-based Production of Polarized Positrons, *SLACProposal-E-166, LC-DET-2003-044;* `http://www.slac.stanford.edu/exp/e166`.
13. H. Olsen and L.C. Maximon, *Phys. Rev.***114**, 887 (1959).
14. H. Schopper, *Nucl. Instr. and Meth.* **3**, 158 (1958); M. Fukuda *et al.*, *Phys. Rev. Lett.***91**, 164801 (2003).

* **List of Authors:**
G. Alexander[DE,TA],P. Anthony[SL],V. Bharadwaj[SL], Y. K. Batygin[SL],T. Behnke[DE,SL],S, C. Berridge[UT], G. R. Bower[SL],W.M. Bugg[UT],R. Carr[SL], E. Chudakov[JL],J. Clarke[DA],J. E. Clendenin[SL], F.-J. Decker[SL],Y. Efremenko[UT],T. Fieguth[SL], K. Flöttmann[DE],M. Fukuda[TO],V. Gharibyan[DE], T. Handler[UT],C. Hast[SL],T. Hirose[WA],R. H. Iverson[SL], Y. Kamychkov[UT],H. Kolanoski[HU],K. Laihem[DE], T. Lohse[HU],C. Lu[PR],K. T. McDonald[PR], N. Meyners[DE],R. Michaels[JL],A. A. Mikhailichenko[CO], K. Mönig[DE],G. Moortgat-Pick[DU],M. H. Munro[SL], M. Olson[SL],T. Omori[KE],D. Onoprienko[BR], N. Pavel[HU],R. Pitthan[SL],R. Poeschl[DE], S. Riemann[DE],L. Rinolfi[CE],K.-P. Schüler[DE], D. Scott[DA],T. Schweizer[HU],J. C. Sheppard[SL] S. Spanier[UT],A. Stahl[DE],Z. M. Szalata[SL],J. Turner[SL], D. Walz[SL],A. W. Weidemann[SC],J. Weisend[SL]

[BR] Brunel University, Uxbridge, Middlesex UB8 3PH, United Kingdom; [CE] CERN, CH-1211 Geneva 23, Switzerland; [CO] Cornell University, Ithaca, NY 14853; [DA] Daresbury Laboratory,Daresbury, Warrington, Cheshire, United Kingdom; [DE] DESY, D-22603 Hamburg, Germany; [DU] University of Durham, Durham DH1 3HP, United Kingdom; [JL] Thomas Jefferson National Accelerator Facility, Newport News, VA 23606; [HU] Humboldt University, Berlin, Germany; [KE] KEK, Tsukuba-shi, Ibaraki, Japan; [PR] Joseph Henry Laboratory, Princeton University, Princeton, NJ 08544; [SC] University of South Carolina, Columbia, SC 29208; [SL] Stanford Linear Accelerator Center, Stanford, CA 94309; [TA] University of Tel Aviv, Tel Aviv 69978, Israel; [TO] Tokyo Metropolitan University, Hachioji-shi, Tokyo, Japan; [UT] University of Tennessee, Knoxville, TN 37996; [WA] Waseda University, 389-5 Shimooyamada-machi,Machida,Tokyo 194-0202.